TECHNICAL NOTES

NATIONAL ADVISORY COMMITTEE FOR AERONAUTICS

No. 739

A RECURRENCE FORMULA FOR SHEAR-LAG PROBLEMS

By Paul Kuhn
Langley Memorial Aeronautical Laboratory

Washington
December 1939

NATIONAL ADVISORY COMMITTEE FOR AERONAUTICS

TECHNICAL NOTE NO. 739

A RECURRENCE FORMULA FOR SHEAR-LAG PROBLEMS

By Paul Kuhn

SUMMARY

The analysis of the bending action in box beams with appreciable shear deformation of the flanges becomes very difficult in the general case of variable cross section and loading. This paper presents a convenient method of solving the problem by the familiar method of dividing the beam into a number of bays that can be assumed to have constant cross section and loading. Application of formerly derived shear-lag formulas leads to a general equation closely analogous in form to the well-known three-moment equation. A numerical example and two comparisons between calculation and experimental results are included.

INTRODUCTION

In the sheet-stringer combinations typical of present-day aircraft construction, the distribution of the stresses is materially influenced by the shear deformation of the sheet. A basic theory for this "shear-lag" problem was discussed in reference 1 and the analysis of single-stringer structures, such as shown in figure 1, was included for simple cases. Reference 2 showed that the additional mathematical difficulties introduced by multi-stringer structures, such as shown in figure 2, could be circumvented by using "substitute single-stringer structures."

The analysis of even a single-stringer structure, however, presents difficulties in the general case, in which the cross section as well as the loading may vary along the length of the structure. In reference 3 were discussed various methods of dealing with this problem by means of numerical integration methods. These methods furnish a comparatively simple solution, considering the complexity of the problem, but they are inadequate for taking into account all the possible variations of parameters. One result of this weakness is that the solutions may be reliable only near the root of the beam, a serious drawback in all of the cases where it is not certain that the critical section will be near the root. For such cases, mathematically more rigorous methods of solution are desirable. A principle for such a method was given in reference 1 in a very brief form; the present paper shows in detail the most convenient manner of setting up the equations and also shows comparisons of theory with test data.

BASIC ASSUMPTIONS AND SIMPLIFICATIONS

For the sake of completeness, the basic assumptions and methods of procedure will be summarized.

The beam is idealized by assuming each stringer together with a certain effective width of sheet to be concentrated at its centroid. The resulting idealized stringers are assumed to carry only longitudinal stresses.

The sheet is assumed to carry all the shear. When the sheet buckles, allowances must be made for the reduced shear modulus. When reasonably heavy stringers are attached to the sheet by two rows of rivets, it is sufficiently accurate to consider only the "free" width of sheet as being subjected to shear deformation.

The transverse stiffness E_y of the cover is assumed to be infinite.

The shear stiffness G of shear webs in beams is assumed to be infinite.

For a beam with a number of stringers, which is the usual case, the stringers are replaced by a single "substitute" stringer (reference 2).

The material on the side opposite to the one being analyzed is, in general, assumed to be concentrated into a compact flange attached directly to the shear web, converting the closed box into an open box. For example, when the tension side of the beam is being analyzed, all the compression material is assumed to be concentrated into a flange attached to the shear web. The effective centroid for this flange may be estimated, with some allowance being made for shear-lag action, on the basis of experience or of a first calculation. Typical cross sections of the resulting substitute single-stringer beams are shown in figures 3(a) and 3(b). As indicated by the dotted lines, the beams are assumed to be symmetrical about a longitudinal plane so that only one-half of the structure needs to be analyzed.

The substitute beam gives the stresses in the corner flange of the actual multistringer beam. The calculation of the normal stresses in the stringers and of the shear stresses in the sheet of the actual beam is dealt with in reference 2.

All calculations given in this paper deal only with single-stringer beams. The subscript S denoting substitute (reference 2) is therefore omitted as unnecessary.

More detailed discussions of these assumptions and of the basic theory, as well as the symbols and the sign conventions used, will be found in references 1 and 2.

GENERAL PRINCIPLES OF ANALYSIS

Direct analytical solutions of the shear-lag problem have thus far been given only for simple cases. References 1 and 2 give solutions for beams in which the cross section is constant and the running shear in the web S_W/h_W is constant.

Actual beams will usually have a variable cross section and loading. Numerical solutions for such cases are obtained by a familiar expedient: The beam is divided into a number of bays so that no appreciable error is committed by assuming that the cross section and the running shear in the web are constant within each bay. The known analytical solutions can then be applied to each individual bay.

The complete numerical solution requires the knowledge of $(r + 1)$ boundary conditions for a beam with r bays. Two of these conditions are furnished by the known conditions at the ends of the beam, the root, and the tip. The remaining conditions are furnished by the principle of elastic continuity, which requires that the elastic deformation at the outboard end of any bay must equal the elastic deformation at the inboard end of the next bay adjoining it.

DERIVATION OF EQUATIONS FOR BEAMS WITH FLAT COVER AND CONSTANT WIDTH AND DEPTH

The beam is divided into bays as shown in figure 4, and the bays and the stations are numbered as indicated. Figure 5 shows the two adjacent cells n and $n + 1$ as free bodies on which the forces act. For the derivation of the equations, it will be assumed that the upper side of the beam is being analyzed for shear-lag effects; the lower side is therefore assumed to be concentrated into a flange attached to the shear web.

In figure 6, the flange and the longitudinal stringer forces F_F and F_L are separated into two groups of forces:

(1) The group of forces shown in figure 6(a), denoted by the superscript P indicating that these forces are calculated by the ordinary bending theory, which assumes that plane cross sections remain plane and (tacitly) that the shear modulus is infinite.

(2) The group of forces X shown in figure 6(b) representing the changes in stringer forces caused by shear deformation of the cover sheet.

Since the first group of forces is in equilibrium by itself, the second group must also be in equilibrium by itself; that is, the force X_F acting on the flange at any given station must be equal and opposite to the force X_L acting on the longitudinal at the same station. This result was anticipated in figure 6(b) by omitting the subscripts F and L from X.

The chief reason for separating the forces into the P-group and the X-group is economy of arithmetic. The statically indeterminate calculation of the shear-lag effects furnishes corrections only to the stresses computed by the ordinary bending theory and can therefore be carried through with a lesser degree of accuracy than would be required if the total forces were chosen as statically indeterminate unknowns.

The groups of forces acting on each bay are associated with shear forces in the cover sheet. The deformations caused by these shear forces will be calculated for the inboard end of bay n and for the outboard end of bay $n + 1$. If the two deformations are equated in accordance with the principle of elastic continuity, a general expression will be obtained that will relate the X-forces at three successive stations with the properties of the two bays between these stations.

Figure 7 shows the cover of bay n with the forces acting on it separated into groups. The P-group calculated by the ordinary bending theory is shown in figure 7(a). The shear stress accompanying this group causes the shear deformation $\gamma_{n_i}{}^{P}$ at the inboard end of the bay as indicated, the superscript P indicating the force group causing the deformation and the sub-subscript i denoting the inboard end. Figure 7(b) shows the X_n-group acting at the inboard end of the bay. The shear stresses associated with this group cause the shear deformation $\gamma_{n_i}{}^{X_n}$. Figure 7(c) shows the X_{n-1}-group acting at the outboard end of the bay; the shear stresses associated with this group cause the shear deformation $\gamma_{n_i}{}^{X_{n-1}}$ at the inboard end. The total shear deformation at the inboard end of bay n is

$$\gamma_{n_i} = \gamma_{n_i}{}^{P} + \gamma_{n_i}{}^{X_n} + \gamma_{n_i}{}^{X_{n-1}} \qquad (1)$$

Similarly, the shear deformation at the outboard end of bay $n + 1$ is

$$\gamma_{(n+1)_o} = \gamma_{(n+1)_o}{}^{P} + \gamma_{(n+1)_o}{}^{X_n} + \gamma_{(n+1)_o}{}^{X_{n+1}} \qquad (2)$$

where the sub-subscript o denotes the outboard end. The familiar formula $\tau = \frac{SQ}{tI}$ of the ordinary bending theory gives

$$\gamma_i{}^{P} = \gamma_o{}^{P} = \gamma^{P} = \frac{\tau}{G_e} = \frac{S_W A_L}{h_W t A_T G_e} \qquad (3)$$

The numerical values of this deformation can be computed for each bay, using average values for the individual factors.

By application of formulas (B-8) of reference 1, and introducing new symbols p and q for convenience, it is found that

$$\gamma_{n_i}^{X_n} = -X_n \frac{K_n}{t_n\, G_{e_n}\, \tanh(KL)_n} = -X_n\, p_n \tag{4}$$

$$\gamma_{n_i}^{X_{n-1}} = X_{n-1} \frac{K_n}{t_n\, G_{e_n}\, \sinh(KL)_n} = X_{n-1}\, q_n \tag{5}$$

$$\gamma_{(n+1)_o}^{X_n} = X_n \frac{X_n\, K_{n+1}}{t_{n+1}\, G_{e_{n+1}}\, \tanh(KL)_{n+1}} = X_n\, p_{n+1} \tag{6}$$

$$\gamma_{(n+1)_o}^{X_{n+1}} = -X_{n+1} \frac{K_{n+1}}{t_{n+1}\, G_{e_{n+1}}\, \sinh(KL)_{n+1}} = -X_{n+1}\, q_{n+1} \tag{7}$$

In these formulas, $A_T = A_F + A_L$, and the parameter K is defined by

$$K^2 = \frac{G_e t}{E\, b}\left(\frac{1}{A_F} + \frac{1}{A_L}\right) \tag{8}$$

Substituting the expressions (4) to (7) into (1) and (2) and equating γ_{n_i} to $\gamma_{(n+1)_o}$ give the general relation

$$X_{n-1}\, q_n - X_n(p_n + p_{n+1}) + X_{n+1}\, q_{n+1} = -\gamma_n^P + \gamma_{n+1}^P \tag{9}$$

which is the basic recurrence formula for the shear-lag problem. The unknown forces X are obtained by solving a system similar to the familiar system of three-moment equations; i.e., a system of n equations, each equation except the last one and usually the first one involving three unknowns.

BOUNDARY CONDITIONS

The first equation of the system is

$$X_o q_1 - X_1(p_1 + p_2) + X_2 q_2 = -\gamma_1 + \gamma_2 \qquad (10)$$

If only transverse loads are applied to the shear web (fig. 8(a)),

$$X_o = 0$$

If a couple $P\ h_W$ is introduced at the tip of the shear web (fig. 8(b)), then

$$X_o = P\frac{A_L}{A_T} \qquad (11)$$

The last equation of the system is

$$X_{r-1} q_r - X_r p_r = -\gamma_r + \gamma_{r+1} \qquad (12)$$

In this equation, γ_{r+1} is the "equivalent" shear deformation of the foundation to which the beam is attached. This deformation is defined by

$$\gamma_{r+1} = \frac{\delta}{b} \qquad (13)$$

where δ is the relative longitudinal displacement of the root fittings at the flange F and at the longitudinal L.

The conditions at the root will fall under one of three classifications:

(1) Rigid foundation.- Although a perfectly rigid foundation is physically impossible, the foundation may be stiff enough to be considered rigid, and the displacement δ will be zero. In practical cases, the condition of zero displacement may be obtained by symmetry of the beam about the plane of station r.

(2) Foundation yielding elastically or inelastically.- The case of a foundation that yields elastically or inelastically occurs, for instance, when the stresses in a wing

are carried through the fuselage by transverse members; the elongation of these members under load permits relative displacements δ of the root fittings on the wing. These displacements may be obtained by successive approximation; in the case of elastic yielding, a carry-through member may be treated as an additional bay of the beam, adding one unknown and one equation to the system.

(3) Longitudinal free at the root.- The case of the longitudinal that is unconnected at the root occurs, for instance, at the tension side of a beam when the stringers butt against the center section but are unconnected to it (or when the connection is too flexible to be taken into account structurally). In this case, the last equation of the system disappears, and X_r is determined by static considerations to be

$$X_r = \frac{M}{h_W} \frac{A_L}{A_T} \qquad (14)$$

BEAM WITH CAMBERED COVER AND TAPER IN DEPTH AND WIDTH

The basic formulas given in the preceding sections require some modifications when the cover is cambered, when the beam is tapered in depth, in width, or in both.

In a beam with cambered cover as shown in figure 3(b), the parameter K is defined by (reference 2)

$$K^2 = \frac{G_e t}{E b'} \left(\frac{1 + \frac{c}{h_W}}{A_F} + \frac{1}{A_L} \right) \qquad (15)$$

In addition to the X-group, it is necessary, for reasons of static equilibrium, to introduce also a group of forces $X\frac{c}{h_W}$ acting as shown in figure 9. These forces do not appear in the statically indeterminate calculation because they do not cause shear deformation of the cover; they must be taken into account, however, when the stresses in the flanges are computed.

In a beam with a flat cover, shear-lag action in the flat-cover side of the beam does not change the total force on the opposite side of the beam at any given station; for instance, shear-lag action on the tension side does not change the total force on the compression side if the tension side has a flat cover. Shear-lag action on a cambered cover, however, does change the total force on the opposite side of the beam by the amount $X\frac{c}{h_W}$ because the shift of force between the longitudinal and the flange on the cambered side reduces the effective depth of the beam.

In a beam with cambered covers on both sides (fig. 10) and with cross sections symmetrical about both axes, it is obviously unnecessary to analyze one side of the beam at a time; the conversion of the closed box into an open box by combining all the material on one side into a single flange attached to the web is therefore omitted. The parameter K is defined by

$$K^2 = \frac{G_e t}{Eb'}\left(\frac{1 + \frac{2c}{h_W}}{A_F} + \frac{1}{A_L}\right) \qquad (16)$$

and the additional force group acting on the upper and the lower corner flanges is $X\,\frac{2c}{h_W}$.

In a beam with cambered cover, the basic equation (3) must be written in the more general form

$$\gamma^P = \frac{SA_L z_L}{G_e\ It} = \frac{S\ Q_L}{G_e\ It} \qquad (17)$$

Also, equations (11) and (14) for the boundary conditions must be written in the more general form

$$X_o = Ph_W\,\frac{Q_L}{I} \qquad (11a)$$

and

$$X_r = \frac{MQ_L}{I} \qquad (14a)$$

In a beam tapered in depth, the shear S in equations (3) and (17) must be understood to be the difference between the external shear and the vertical components of the stringer forces as given by the familiar formula

$$S = S_E - \frac{M}{h} \tan \delta \tag{18}$$

where h is the effective depth of the beam and δ is the inclination between the effective compression flange and the effective tension flange. For a beam with cambered cover, equation (18) may be written in the more general form

$$S = S_E - \frac{MQ}{I} \tan \delta \tag{19}$$

where Q is the static moment of A_F and A_L about the centroidal axis.

Serious theoretical difficulties arise when the beam has taper in width. The method of analysis developed thus far may be considered dependent upon two distinct basic theories: the engineering theory of bending and the simplified theory of shear deformation in a skin-stringer combination. Both theories break down when the beam has taper in width, so that the development of an entirely rational theory is impossible without utilizing or developing considerably more refined basic theories.

As a temporary solution for engineering purposes, a semirational modification of the procedure for beams with constant width may be used. The actual width b and the actual thickness t of the sheet are replaced by a fictitious width b_f and a fictitious thickness t_f. The fictitious width at any given station is taken as

$$b_f = b \left(\frac{b_o}{b}\right) = b_o \tag{20}$$

where b is the actual width at the station and b_o the actual width at the root; the introduction of this fictitious width converts the tapered beam into a beam of constant width equal to the width at the root of the tapered beam.

The fictitious thickness t_f at any station may be so determined that the shear stiffness of the fictitious sheet will equal the shear stiffness of the actual sheet at that station. Because the shear stiffness of the sheet is proportional to t/b, this method of procedure would require that

$$t_f = t \frac{b_o}{b} \tag{21}$$

The use of this fictitious thickness then compensates for the use of a fictitious width; at any station along the span, the shear-lag parameter K of the fictitious beam with constant width equals the parameter K of the actual beam with tapered width. The coefficients $\bar{p}_n$, $\bar{q}_n$, and $\bar{\gamma}_n$, as defined by equations (3) to (7), are changed because they involve t independently of b.

Considerations of the limiting case of a beam tapered to a point tend to indicate that this method of compensation is inadequate, and comparison with the tests of N.A.C.A. beam 4 described in reference 2 shows rather poor agreement. More satisfactory agreement between this test and calculation is obtained when the fictitious thickness is taken as

$$t_f = t \left(\frac{b_o}{b}\right)^2 \tag{22}$$

The use of this value for the fictitious thickness changes not only the coefficients p, q, and γ but also the shear-lag parameter K at each station.

Physically, the use of equations (20) and (21) may be interpreted as taking into account only the direct effect of variable width on the shear stiffness and neglecting all the effects of transverse components of forces caused by the inclination of the flange toward the center stringer. The use of equation (22) represents an attempt to take into account the effect of this inclination of the flange.

COMPARISON BETWEEN CALCULATION AND TEST RESULTS

Only two tests are available for checking the method of analysis developed. One already mentioned is that of N.A.C.A. beam 4 described in reference 2. The second one is described in reference 4. The beam used in the second test had a constant cross section, but the load was applied in the form of several concentrated loads. Figure 11 shows the experimental and the calculated results for N.A.C.A. beam 4; figure 12 shows the results for the beam of reference 4. As a matter of some interest, the u-solution of reference 3, as well as the X-solution of this paper, is shown in these figures.

The agreement between test and calculation is not all that could be desired for N.A.C.A. beam 4. It is possible that some of the discrepancy near the root was caused by defective workmanship in one flange, which may be the reason for the decided drop in stress of one flange near the root. Regardless of whether defective workmanship in the flange caused the discrepancy, an experimental check of the specific influence of taper in width appears desirable.

The agreement for the beam of figure 12 is very much better, particularly in the critical region near the root. The X-solution predicts correctly, at least qualitatively, the reversal in stress near the tip; the u-solution does not. The u-solution depends on the total shear at the root and gives a very good approximation near the root; it cannot take into account the manner in which the load is distributed along the span and, concomitantly, it cannot be expected to give results in very close agreement with the facts outboard of the root region, particularly if there are discontinuities of loading or cross section. Whether such disagreement is of practical importance depends, of course, on the individual circumstances.

Langley Memorial Aeronautical Laboratory,
National Advisory Committee for Aeronautics,
Langley Field, Va., November 16, 1939.

APPENDIX

Numerical Example

As a numerical example for the method of analysis developed, the analysis of N.A.C.A. beam 4 will be given. The dimensions of this beam are given in reference 2. The single-stringer beam substituted for the actual beam is calculated by the method described in reference 2 as follows:

The compression flanges, the tension flanges, and the longitudinals are assumed to be concentrated at their respective centroids. The cover sheet, which is 0.0114 inch thick, is assumed to be fully effective in aiding the longitudinals, and the adjacent strips of sheet are added to the longitudinals or flanges. The shear web is also assumed to be fully effective in bending and is replaced by concentrated flanges of cross-sectional area 1/6 A_W. The area of the substitute longitudinal is calculated by formula (4) of reference 2:

$$A_{LS} = A_L \frac{\sinh K_3 b}{K_3 b}$$

The substitute camber is taken as

$$c_S = \frac{1}{2} c$$

The subscript S is dropped as unnecessary for the present paper. With the geometrical properties of the single-stringer substitute beam thus defined and listed in rows 1 to 5 of table I, the average section modulus I/z_L can be computed for each bay and is listed in row 6.

The effect of taper in width is allowed for by introducing the fictitious width b_f and the fictitious sheet thickness t_f, according to formulas (20) and (22); the shear-lag parameter is then calculated by the formula

$$K^2 = \frac{Gt_f}{Eb_f'}\left(\frac{1 + \frac{c}{h_W}}{A_F} + \frac{1}{A_L}\right) = \frac{Gt}{Eb'}\,\frac{b_o'}{b'}\left(\frac{1 + \frac{c}{h_W}}{A_F} + \frac{1}{A_L}\right)$$

and listed in row 7; KL is then listed for each bay, L being 19 inches for each bay, and the values of KL, sinh KL, and tanh KL are found in rows 8, 9, and 10, respectively.

The next step is the computation of the coefficients p, q, and γ for the system of X-equations. Some slight modifications were made in this particular case to reduce the amount of arithmetic. The shear modulus G appears as a factor in all coefficients and consequently can be canceled. The thickness t_f for all bays involves the thickness t as a common factor, so that t can be canceled. With these modifications, the coefficients become

$$p = \frac{K}{\tanh KL} \frac{b'}{b_o'}$$

$$q = \frac{K}{\sinh KL} \frac{b'}{b_o'}$$

and are listed in rows 11 and 12.

Before the coefficient γ is computed, the shear for each bay must be computed by formula (18) or (19); the load is a concentrated load of 250 pounds applied at the tip, and the resulting shear S is listed in row 13. With this shear S and by the use of the modifications previously mentioned, the coefficient γ^P is

$$\gamma^P = \frac{SQ_L}{I} \frac{b}{b_o}$$

and is listed in row 14.

With these coefficients, the system of equations formed according to the general equation (9) is

$$\begin{array}{llllll}
 & -0.0791\ X_1 & +0.01354\ X_2 & & = & 0.04 \\
0.01354\ X_1 & -0.0921\ X_2 & +0.02068\ X_3 & & = & 0.06 \\
0.02068\ X_2 & -0.1070\ X_3 & +0.02908\ X_4 & & = & 0.02 \\
0.02908\ X_3 & -0.1248\ X_4 & +0.0383\ \ X_5 & & = & 0.02 \\
0.0383\ \ X_4 & -0.0373\ X_5 & & & = & -14.90
\end{array}$$

The solution of this system of equations gives the values of X listed in row 1 of table II. The flange stresses caused by the X-group are

$$\sigma_X = \frac{X}{A_F}\left(1 + \frac{c}{h_W}\right)$$

and are listed in row 2 of table II. This tabulation completes the X-solution of the substitute beam. The total flange stresses σ in the actual beam are found by adding the stresses σ_X to the flange stresses σ_P, calculated for the actual beam by the ordinary bending theory, as shown in rows 3 and 4 of table II. Figure 11 shows the results graphically. Strictly speaking, the stresses within each bay should be calculated by using formulas (B-8) of reference 1 or (A-3) of reference 2; this refinement, however, is seldom necessary.

REFERENCES

1. Kuhn, Paul: Stress Analysis of Beams with Shear Deformation of the Flanges. T.R. No. 608, N.A.C.A., 1937.

2. Kuhn, Paul: Approximate Stress Analysis of Multistringer Beams with Shear Deformation of the Flanges. T.R. No. 636, N.A.C.A., 1938.

3. Kuhn, Paul: Some Notes on the Numerical Solution of Shear-Lag and Mathematically Related Problems. T.N. No. 704, N.A.C.A., 1939.

4. Schapitz, E., Feller, H., and Köller, H.: Experimental and Analytical Investigation of a Monocoque Wing Model Loaded in Bending. T.M. No. 915, N.A.C.A., 1939.

TABLE I

Basic Properties of Beam and Coefficients

for Recurrence Formula

	Bay	1	2	3	4	5
1	A_F	0.1465	0.1535	0.1600	0.1665	0.1735
2	A_L	.330	.395	.460	.525	.590
3	b'	6.71	7.93	9.15	10.37	11.59
4	h_W	3.00	3.60	4.20	4.80	5.40
5	c	.615	.725	.840	.955	1.070
6	I/z_L	1.523	2.117	2.805	3.59	4.47
7	K^2	.01392	.00916	.00643	.00471	.00357
8	KL	2.240	1.815	1.520	1.304	1.163
9	sinh KL	4.643	2.988	2.177	1.706	1.443
10	tanh KL	.978	.940	.909	.862	.822
11	p	.0365	.0426	.0495	.0575	.0673
12	q	.00770	.01354	.02068	.02908	.0383
13	S	225.0	187.5	161.0	140.7	125.0
14	γ^P	14.76	14.80	14.86	14.88	14.90

TABLE II

Flange Forces and Stresses

Station		1	2	3	4	5
1	X	0.4	5.0	25.1	89.4	272.5
2	σ_X	3	38	185	631	1847
3	σ_P	1795	2690	2920	3040	3015
4	σ	1798	2798	3105	3671	4862

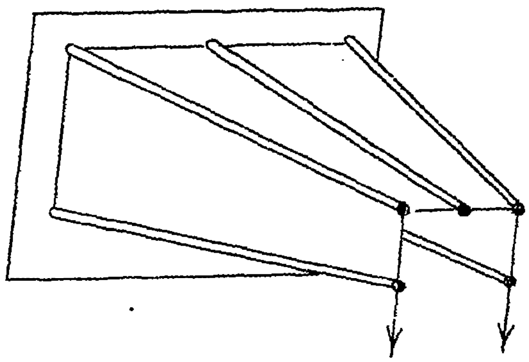

Figure 1.- Single-stringer structure

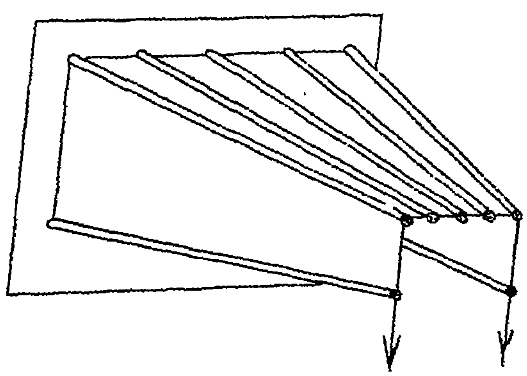

Figure 2.- Multistringer structure.

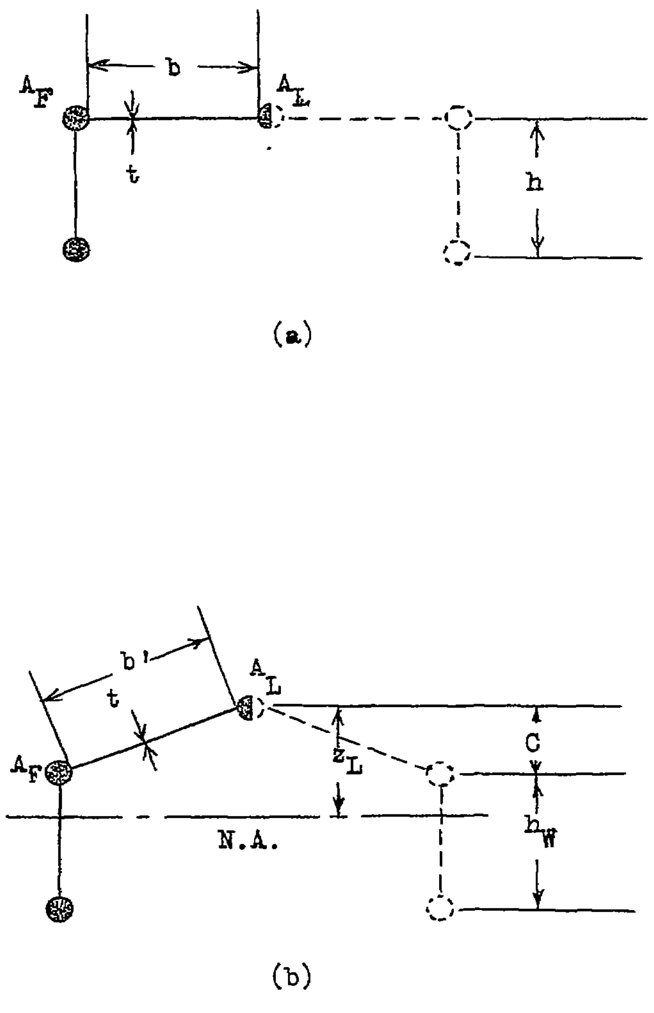

Figure 3.- Typical cross sections of substitute single-stringer beams.

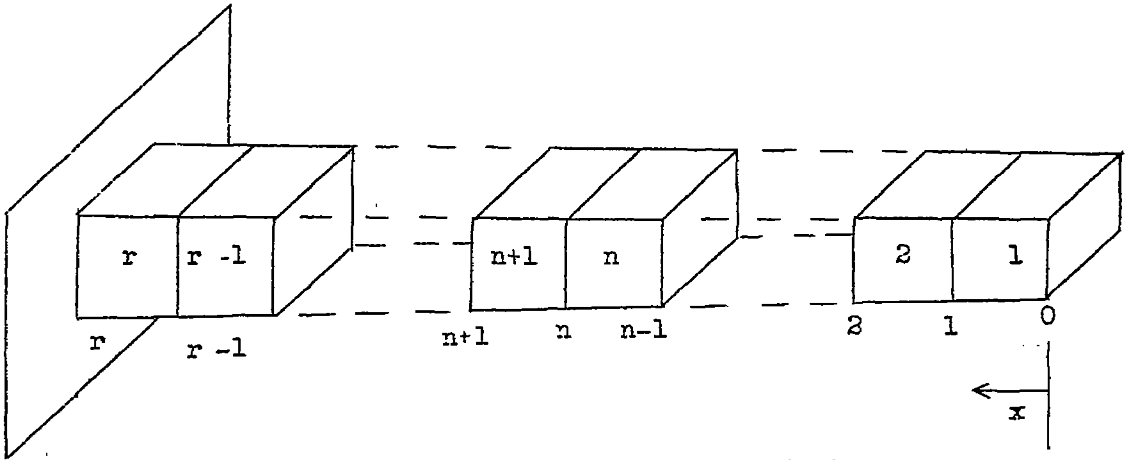

Figure 4.- Division of beam into bays.

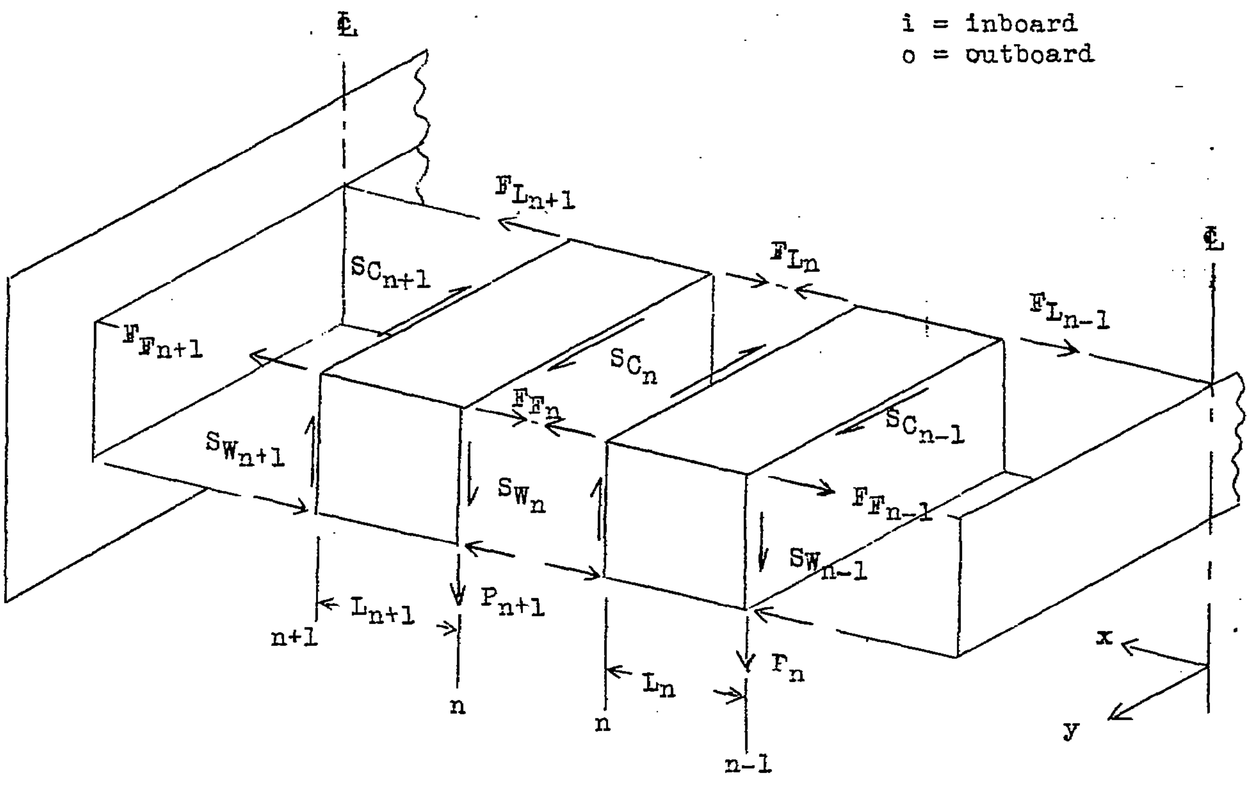

Figure 5.- Forces acting on individual bays.

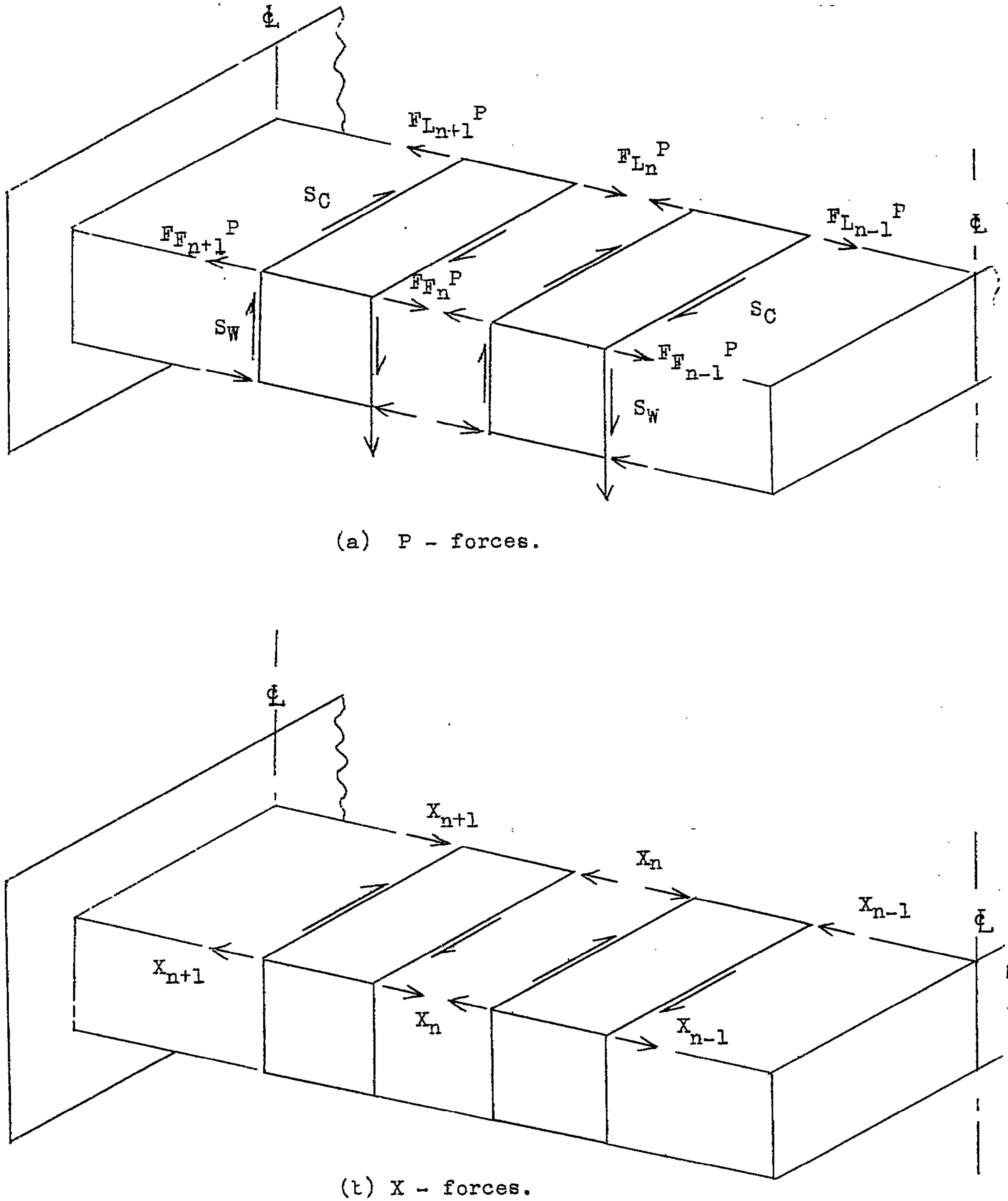

Figure 6.- Division of forces into P - forces and X - forces.

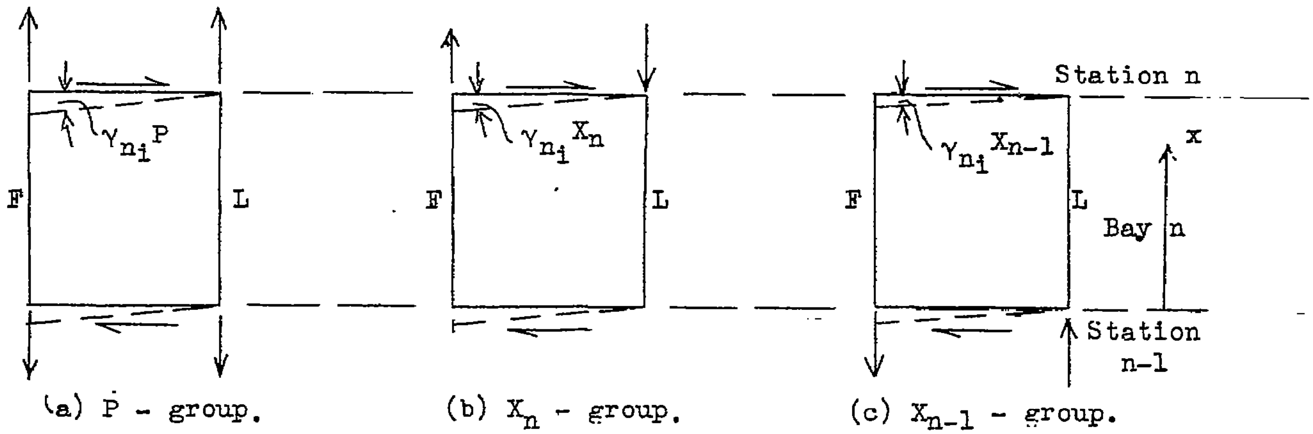

Figure 7.- Forces and deformations on cover of bay n. All forces and deformations are shown as positive.

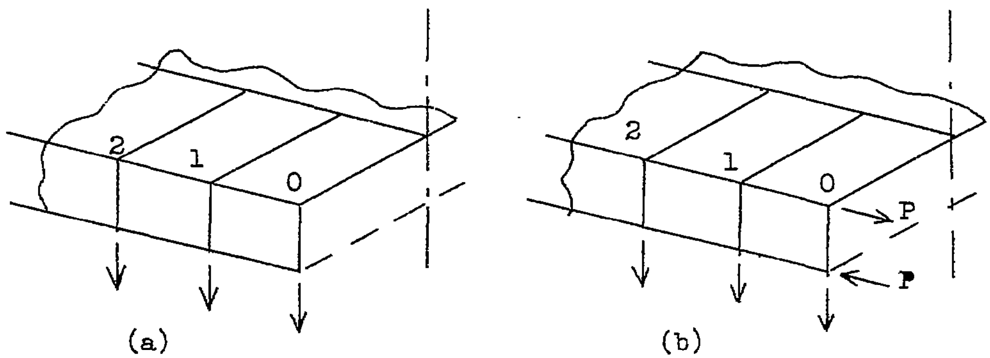

Figure 8.- Types of loading at tip bay.

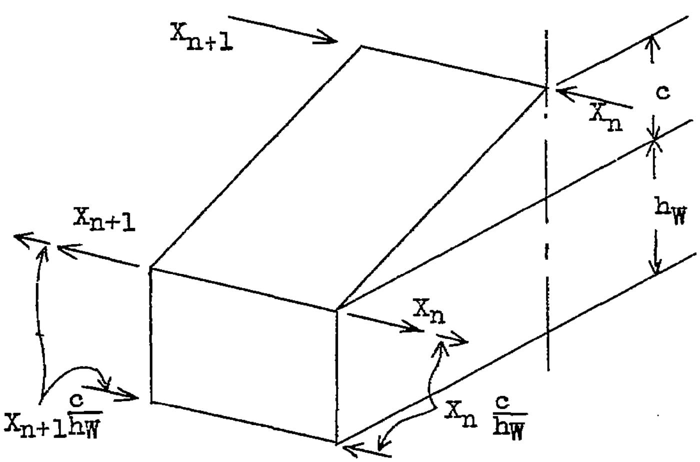

Figure 9.- Group of X - forces on cambered beam.

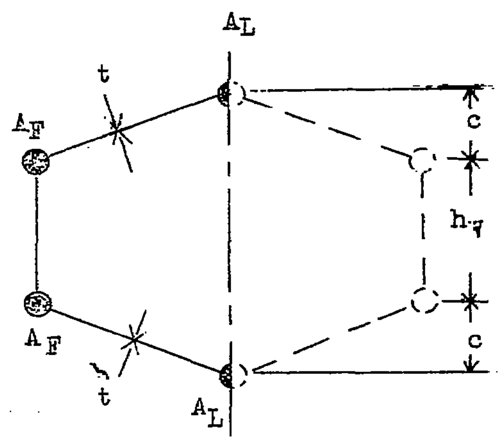

Figure 10.- Beam with both sides cambered.

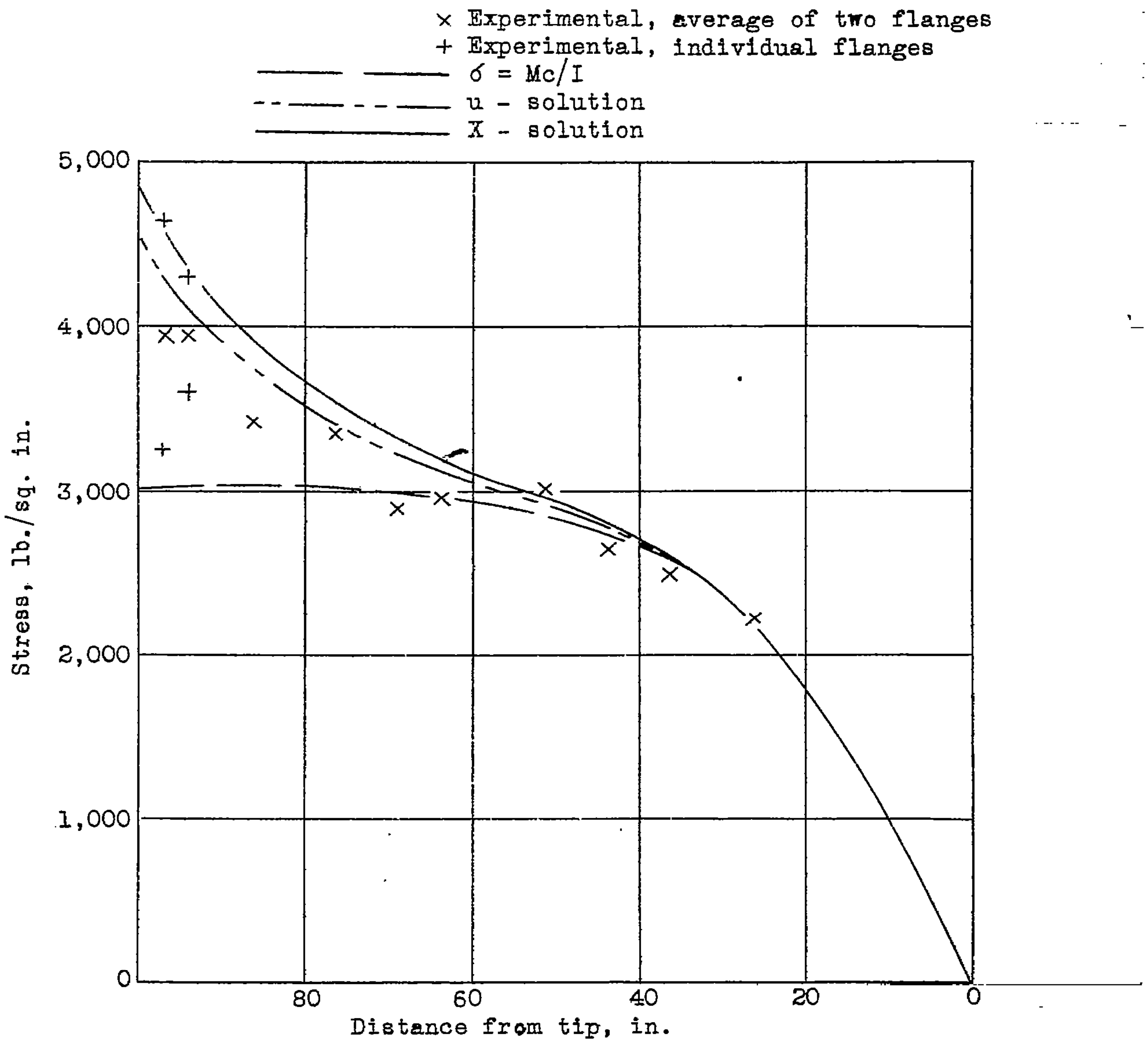

Figure 11.- Flange stresses in tapered beam with tip load. Experimental data from reference 2.

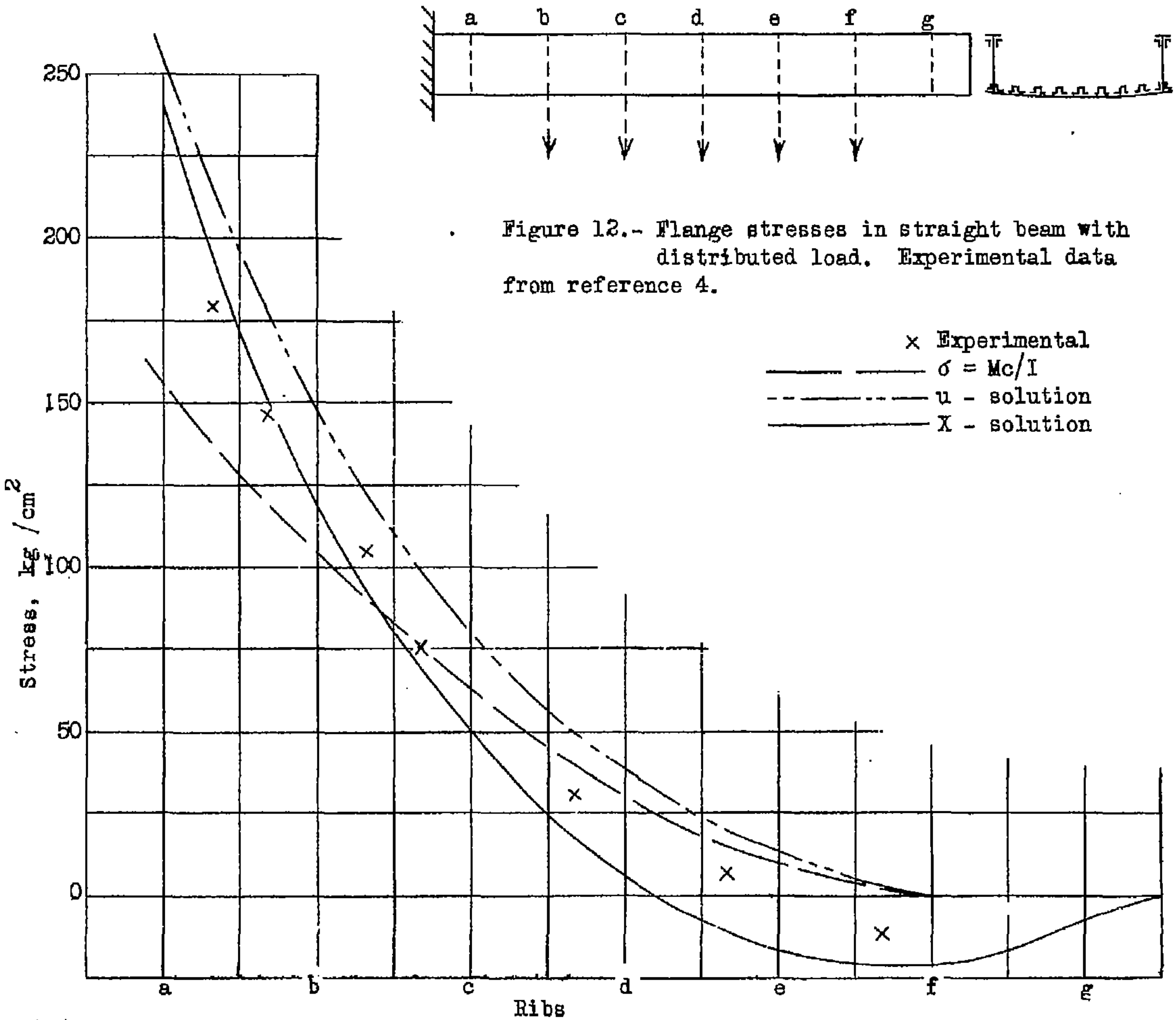

Figure 12.- Flange stresses in straight beam with distributed load. Experimental data from reference 4.